

Learning Unknowns from Unknowns: Diversified Negative Prototypes Generator for Few-Shot Open-Set Recognition

Zhenyu Zhang*
School of Computer Science and
Technology, Huazhong University of
Science and Technology
Wuhan, China
m202273680@hust.edu.cn

Guangyao Chen*
National Key Laboratory for
Multimedia Information Processing,
School of Computer Science, Peking
University
Beijing, China
gy.chen@pku.edu.cn

Yixiong Zou†
School of Computer Science and
Technology, Huazhong University of
Science and Technology
Wuhan, China
yixiongz@hust.edu.cn

Yuhua Li†
School of Computer Science and
Technology, Huazhong University of
Science and Technology
Wuhan, China
idcliuhua@hust.edu.cn

Ruixuan Li
School of Computer Science and
Technology, Huazhong University of
Science and Technology
Wuhan, China
rxli@hust.edu.cn

ABSTRACT

Few-shot open-set recognition (FSOR) is a challenging task that requires a model to recognize known classes and identify unknown classes with limited labeled data. Existing approaches, particularly Negative-Prototype-Based methods, generate negative prototypes based solely on known class data. However, as the unknown space is infinite while the known space is limited, these methods suffer from limited representation capability. To address this limitation, we propose a novel approach, termed **Diversified Negative Prototypes Generator (DNPG)**, which adopts the principle of "learning unknowns from unknowns." Our method leverages the unknown space information learned from base classes to generate more representative negative prototypes for novel classes. During the pre-training phase, we learn the unknown space representation of the base classes. This representation, along with inter-class relationships, is then utilized in the meta-learning process to construct negative prototypes for novel classes. To prevent prototype collapse and ensure adaptability to varying data compositions, we introduce the Swap Alignment (SA) module. Our DNPG model, by learning from the unknown space, generates negative prototypes that cover a broader unknown space, thereby achieving state-of-the-art performance on three standard FSOR datasets. The repository of this project is available at <https://github.com/iCGY96/DNPG>.

*Equal Contribution.

†Corresponding authors.

Permission to make digital or hard copies of all or part of this work for personal or classroom use is granted without fee provided that copies are not made or distributed for profit or commercial advantage and that copies bear this notice and the full citation on the first page. Copyrights for components of this work owned by others than the author(s) must be honored. Abstracting with credit is permitted. To copy otherwise, or republish, to post on servers or to redistribute to lists, requires prior specific permission and/or a fee. Request permissions from permissions@acm.org.

ACM MM, 2024, Melbourne, Australia

© 2024 Copyright held by the owner/author(s). Publication rights licensed to ACM.

ACM ISBN 978-1-4503-XXXX-X/18/06

<https://doi.org/10.1145/3664647.3680646>

CCS CONCEPTS

• **Computing methodologies** → **Computer vision**.

KEYWORDS

Few-shot, Open-set, Learning unknowns from unknowns, Negative-Prototype-Based, Diversified negative prototypes

ACM Reference Format:

Zhenyu Zhang, Guangyao Chen*, Yixiong Zou, Yuhua Li†, and Ruixuan Li. 2024. Learning Unknowns from Unknowns: Diversified Negative Prototypes Generator for Few-Shot Open-Set Recognition. In *Proceedings of the 32nd ACM International Conference on Multimedia (MM'24)*, October 28-November 1, 2024, Melbourne, Australia. ACM, New York, NY, USA, 13 pages. <https://doi.org/10.1145/3664647.3680646>

1 INTRODUCTION

Deep learning [6, 12, 16, 17, 24, 25, 30] has significantly advanced various domains, largely due to its ability to leverage extensive training data. Conventionally, deep models are trained under the closed-set assumption, where the classes in the training data align with those in the test data. However, real-world scenarios often present more complex challenges. Firstly, acquiring a large volume of labeled data is frequently impractical, especially when data collection is costly or involves sensitive information. For instance, datasets for rare disease diagnosis are typically small, and new users in recommendation systems have limited records. Secondly, models must contend with unknown data that falls outside the scope of training classes, such as online shopping platforms needing to identify and update new user-uploaded products.

To address these challenges, Few-Shot Open-Set Recognition (FSOR) [13, 18, 20, 27, 37, 41, 48] has emerged as a critical task. FSOR demands that a model utilize minimal training data from the support set to effectively recognize the query set, which involves classifying known-class samples and identifying unknown-class samples. This can be viewed as an N+1 classification problem (add an "Unknown" class), as depicted in Figure 1. The FSOR model undergoes pre-training on base classes with ample data, which do

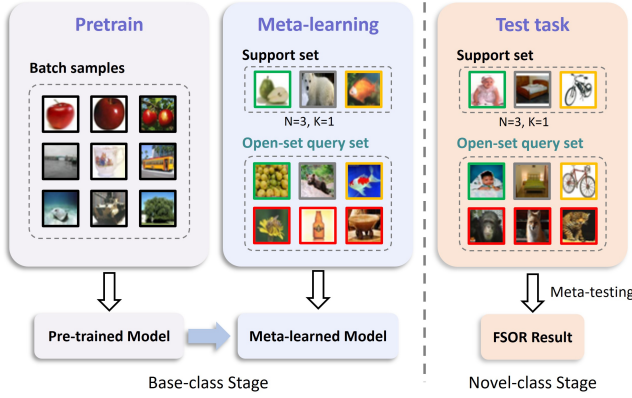


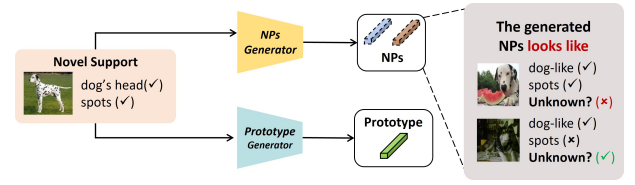
Figure 1: Task setting for FSOR: The model undergoes a two-phase pre-training on base class data, followed by testing where it classifies novel classes (green, gray, orange boxes) and identifies unknown class samples (red box).

not overlap with novel classes, before transitioning to the novel-class stage.

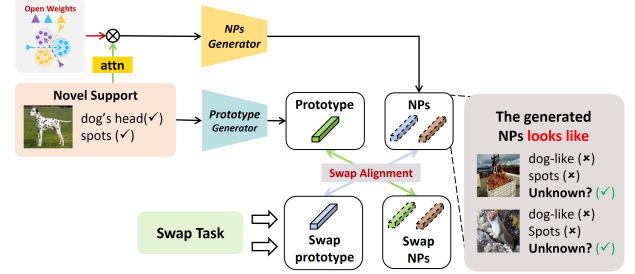
Since the unknown class can be understood as an extra class against known classes, a common strategy is to learn a representation for this unknown class, referred to as the negative prototype (NP), and perform an $N+1$ classification task using the prototypes of both known and unknown classes [7–9]. Existing methods [18, 37, 47] typically generate NPs based on known-class data, as depicted in Figure 2(a). However, this approach inherently limits the diversity of the NPs, as they tend to retain characteristics of the known classes. For instance, an NP generated for the "Dalmatian" class might resemble a generic dog with altered features, failing to represent the vast diversity of the unknown space. The unknown space is theoretically infinite, encompassing a wide range of samples that cannot be directly derived from known classes, such as a guitar being an unknown sample relative to the "Dalmatian" class.

To overcome this limitation, we propose a novel approach to generate diversified NPs by **learning unknowns from unknowns**, thus alleviating the constraints imposed by known-class information. As illustrated in Figure 2(b), during the base-class stage, we leverage extensive data to learn the inverse representation of each base class, which we term the *open weight*. This representation captures the essence of **what is not that class**, effectively representing the corresponding unknown space. During the novel-class stage, utilizing these open weights to generate NPs allows for a broader coverage of the unknown space, enhancing the representation of diverse unknown-class samples. For example, open weights derived from base classes such as cars and planes could correspond to entities like rocks, trees, or the sun, which are unrelated to the given base classes. Consequently, during the novel-class stage, the model can generate diversified NPs for the "Dalmatian" class that are not confined to dog-like animals as shown in Figure 2(b).

However, a challenge arises as the open weights, derived from base classes, remain static during the novel-class stage. This can lead to the generated NPs collapsing into a single point, reducing their effectiveness. To address this, we further introduce the Swap



(a) Existing Negative-Prototype-Based FSOR method.



(b) Our Diversified Negative Prototypes Generator method.

Figure 2: (a) Existing SOTA FSOR methods, like ATT-G [18], generate Negative Prototypes (NPs) from support samples, leading to limited diversity (e.g., "Dalmatian" NPs resemble dog-like animals). (b) Our DNPG model leverages the unknown space representation (open weights) of base classes to produce diversified NPs in the test phase.

Alignment (SA) module, which ensures that NPs model distinct unknown spaces for different novel-class data, thereby preserving their diversity. During the base-class stage, we sample a set of non-overlapping base classes as pseudo-unknown classes and minimize the distance between the generated NPs and these pseudo-unknown classes. Simultaneously, known class samples and pseudo-unknown class samples together form the swap tasks, where, at the prototype level, the distances between NPs and the pseudo-unknown class samples are further reduced. This approach ensures that each generated NP is distinct from all current known-class representations, preventing collapse and enabling adaptation to the current known classes.

In summary, our main contributions are as follows.

- We propose a novel FSOR method, the Diversified Negative Prototypes Generator (DNPG), to generate diversified negative prototypes by learning unknowns from unknowns, using the inverse representation of base classes.
- We introduce the Swap Alignment module to prevent NP collapse and enhance adaptation to novel-class data, further increasing the diversity of NPs.
- Extensive experiments have been carried out on multiple widely used FSOR datasets to prove that our DNPG model is superior to the current state-of-the-art methods.

2 RELATED WORK

Few-Shot Learning. Few-shot learning in visual classification addresses the challenge of classifying with limited support samples. Methods can be broadly categorized into transfer learning,

which leverages pre-trained models from related tasks [39, 43? ? ? ?], and meta-learning, which includes model-based [4, 28], metric-based [15, 36], and optimization-based approaches [1, 19]. Model-based methods adapt quickly to new tasks with minimal data, metric-based methods optimize the distance distribution between samples, and optimization-based methods focus on efficient model training with limited examples.

Open-Set Recognition. Current open-set recognition methods can be categorized based on their approach to discriminating unknown class samples, including similarity threshold-based methods [2, 11, 35], and density threshold-based methods [23, 45]. Additionally, a new trend has emerged, where Gaussian Mixture Models (GMMs) are applied to model closed-set distributions [10, 26], enabling the models to directly reject unknown class samples. However, no previous work has employed GMMs to address the FSOR task. This is mainly attributed to the difficulty of learning the joint distribution of classes and pixel features when only a limited number of labeled samples from the novel classes are available.

Few-Shot Open-set Recognition. FSOR combine the challenges of FSL and OSR, requiring the completion of OSR tasks with limited support samples. PEELER [27] proposes to train and test FSOR tasks in a meta-learning pattern. RFDNet [13] suggests meta-learning a feature displacement relative to a pre-trained reference feature embedding. SnaTCHer [20] identifies unknown samples based on the transformation consistency, which measures the difference between transformed prototypes and a modified prototype set. The GEL [41] model utilizes an energy function as the discriminative criterion and introduces a pixel-level prototype network. ReFOCS [29] adopts a generative approach to dynamically adjust the similarity threshold by reconstructing samples. OPP [38] proposes constructing an overall positive prototype and then filters out unknown class samples using a threshold method. MSCL [46] combines the strengths of supervised contrastive learning and meta-learning to effectively increase inter-class distinctions and reinforce intra-class compactness. MRM [5] proposes enlarging the margin between different classes by extracting the multi-relationship of paired samples to dynamically refine the decision boundary for known classes and implicitly delineate the distribution of unknowns.

Negative-Prototype-Based FSOR Methods. These FSOR methods learn one or multiple prototypes for unknown class samples, thereby transforming the open-set recognition task into an $N+1$ classification task. Existing Negative-Prototype-Based FSOR methods: ProCAM [37] learns NPs by extracting the background of support set images, ATT-G [18] uses attention mechanisms to generate NPs that are distant from known class samples. ASOP [21] proposes to generate a negative prototype closest to open-set samples and second-closest to closed-set samples. TNPNet [44] adopts a transductive learning approach, leveraging both local and global contexts to enhance prototypes and negative prototypes. However, these methods utilize known class samples from the support set to learn NPs, which inevitably leads to the NPs inheriting the characteristics of the known class samples. As a consequence, the learned NPs are limited in their ability to model the unknown space, as illustrated in Figure 2 (a).

Multiple Prototypes Model. This approach involves generating multiple prototypes to represent a batch of data. Methods like [9, 18] generate multiple negative prototypes, but often face

challenges such as prototype collapse and ineffective utilization of prototypes. Some studies [31, 42] attempt to address these issues with an equipartition constraint, but these methods may not perform well in small-sample open-set recognition tasks and could potentially decrease model performance.

3 PRELIMINARIES

3.1 Few-Shot Open-Set Recognition Setting

FSOR task aims to achieve accurate classification of known classes with limited support samples while effectively identifying instances from unknown classes. Formally, an FSOR task \mathcal{T} is defined as a triplet $\mathcal{T} = \{\mathcal{S}, Q_k, Q_u\}$, comprising a support set $\mathcal{S} = \{x_i, y_i\}_{i=1}^{|\mathcal{S}|}$, a query set $Q_k = \{x_i, y_i\}_{i=1}^{|Q_k|}$ for known classes, and an open-set query set $Q_u = \{x_i, y_i\}_{i=1}^{|Q_u|}$ for unknown classes. The support set \mathcal{S} contains K samples per class, where K is typically small (e.g., 1 or 5). The labels y for the support set \mathcal{S} and query set Q_k belong to the set of novel known classes C_k , while the labels for Q_u belong to the set of unknown classes C_u , with $C_k \cap C_u = \emptyset$.

A proficient FSOR model should: (1) accurately classify images from the query set Q_k into the corresponding known classes using the knowledge encapsulated in the support set \mathcal{S} , and (2) effectively recognize images from classes not represented in the current support set (i.e., samples from Q_u) as belonging to unknown classes.

3.2 Negative-Prototype-Based FSOR

Negative-prototype-based FSOR approaches transform the open-set recognition problem into an $(N+1)$ -way closed-set classification task by introducing Negative Prototypes (NPs). In the absence of unknown-class samples, a prototype-based few-shot classifier can be formulated as

$$\arg\max_c \left(\{f_s(\mathcal{F}_\theta(q), \mathbf{p}_c)\}_{c \in C_k} \right), \quad (1)$$

where \mathcal{F}_θ is the feature extractor, f_s is the similarity function, C_k denotes the set of novel known classes, and \mathbf{p}_c represents the prototype for class c , computed as the average feature vector of samples belonging to class c . To accommodate unknown-class samples, Negative-Prototype-Based FSOR models extend the prototype-based classification by learning an additional NP for the unknown classes. The classification then involves $(|C_k| + 1)$ prototypes:

$$\arg\max_c \left(\{f_s(\mathcal{F}_\theta(q), \mathbf{p}_c)\}_{c \in C_k \cup \{\text{unknown}\}} \right), \quad (2)$$

where a sample is classified as belonging to an unknown class if it is most similar to the NP.

However, as illustrated in Figure 2(a), existing approaches often derive NPs based on support samples, inadvertently incorporating information from known classes. This can lead to NPs that closely resemble known classes or highly similar classes (e.g., Dalmatians and Alaskans), which complicates the modeling of unknown classes within the diverse space of unknowns.

4 THE PROPOSED METHOD

In this section, we introduce our approach to tackle the FSOR problem by generating diverse NPs. Our model architecture is depicted in Figure 3. We first describe our baseline model, followed by our

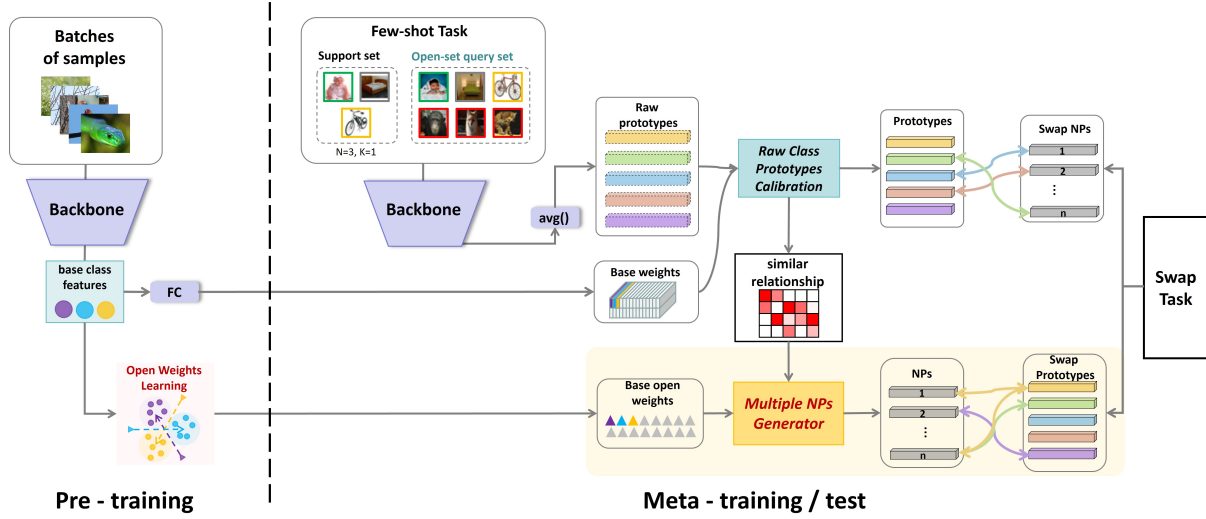


Figure 3: An overview of the base-class stage in our DNPG model. In the pre-training phase, the model learns an inverse representation, termed as open weight, for each base class. During the meta-learning phase, these open weights, along with the similarity relationship between base and novel classes, are utilized to generate Novel Prototypes (NPs). Furthermore, the Swap Alignment module is employed to guide the NP generation process, thereby improving their diversity.

strategy for learning open-set weights for base classes. Finally, we present our Diversified Multiple Negative Prototype Generator (DMNPG) module and the Swap Alignment module, which together facilitate the generation of task-level diversified NPs for different tasks.

4.1 Baseline Model

Our baseline model is built upon the framework proposed by Huang et al. [18] and utilizes a metric-based meta-learning architecture, similar to previous FSOR methods [15, 18, 36]. As shown in Figure 1, the training process is divided into two stages: the base-class stage, which uses a large-scale dataset of base classes, and the novel-class stage, which evaluates the model on a dataset of novel classes with all model parameters fixed.

Pre-training. During pre-training, we employ a ResNet-12 network to perform a large-scale classification task using labeled samples from the base classes. The resulting feature extractor \mathcal{F}_θ and the classifier head for base classes are obtained, with the classifier head weights denoted as P^* .

Meta-learning. In the meta-learning stage, the base class dataset is redivided into different tasks. Sampling 2N classes in each task, with N known classes (\mathcal{S} and \mathcal{Q}_k) and N designated as pseudo-unknown classes (\mathcal{Q}_u). The pre-trained Res-12 network serves as the feature extractor \mathcal{F}_θ to extract low-dimensional feature representations v_i for samples in each task. For each task, the feature representations in the support set are averaged by class to obtain the raw class prototype p_c^r :

$$p_c^r = \frac{1}{K} \sum_{i=1}^K \mathcal{F}_\theta(x_{c,i}^S), \quad v_i = \mathcal{F}_\theta(x_i), \quad (3)$$

where $x_{c,i}^S$ represents the i -th sample of class c from the support set, and $p_c^r \in P^r$ is the raw class prototype of class c , with $c \in \mathcal{C}_S$. A Multi-Layer Perceptron (MLP) is then applied to the averaged

class prototype p_{avg}^- to generate the NP:

$$p^- = f^{mlp}(p_{avg}^-), \quad p_{avg}^- = \frac{1}{|\mathcal{C}_k|} \sum_{c \in \mathcal{C}_k} p_c^r, \quad (4)$$

where p_{avg}^- is the average of the raw class prototypes, considering all novel classes in the current task to generate a task-specific NP.

After obtaining both the raw class prototypes P^r and the NP p^- , the closed-set classification and open-set recognition tasks are combined into a $(|\mathcal{C}_k|+1)$ -way classification task:

$$\arg\max_c \left(\{f_s(\mathcal{F}_\theta(q), [P^r, p^-])\}_{c \in \mathcal{C}_k \cup \text{unknown}} \right), \quad (5)$$

where f_s is a function to measure the similarity between two inputs, e.g., cosine similarity. The cross-entropy loss is used to train the $(|\mathcal{C}_k|+1)$ -way classification baseline model as $\mathcal{L}_{CE}(\mathcal{Q}_k \cup \mathcal{Q}_u)$.

Testing. During the testing phase, the model parameters are fixed. For a test task $\mathcal{T} = \{\mathcal{S}, \mathcal{Q}_k, \mathcal{Q}_u\}$, prototypes of novel classes and the NP are generated using the support set samples \mathcal{S} , as per the equations above. The cosine similarity between the query samples $\{\mathcal{Q}_k, \mathcal{Q}_u\}$ and the prototypes, including the NP, is calculated. A query sample is classified into the corresponding novel class if its cosine similarity with a novel class prototype is the highest. However, if its cosine similarity with the NP is the highest, it is considered to be from an unknown class.

4.2 Diversified multiple NPs generator

Our method aims to generate negative prototypes directly from the unknown space by utilizing the base-class inverse representation, referred to as **open weights**, and leveraging the similarity relationships between classes.

Learning the transferable open weights. In the pre-training phase, we adopt the concept of Reciprocal Prototype Learning (RPL) [9] to learn the open weight O_j for each base class j . The objective is to position O_j far from the samples of class j while

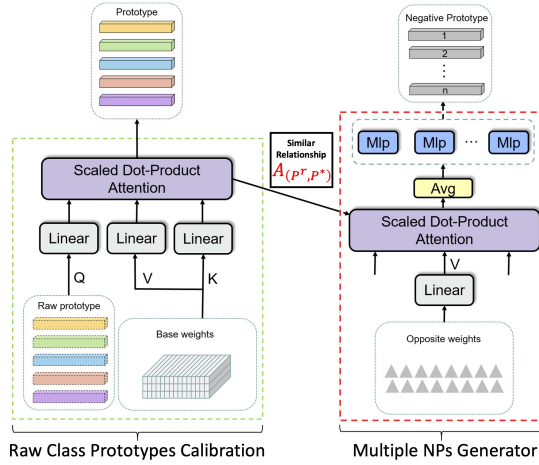


Figure 4: Details of the Raw Class Prototypes Calibration (RPC) and Multiple NPs Generator (MNG) modules. In the RPC module, a standard Transformer attention block is utilized to calibrate raw prototypes with base weights. Subsequently, in the MNG module, based on the similarity relationship established in the RPC module, open weights are employed to generate multiple NPs for the current episode.

maintaining proximity to samples from other base classes. This is achieved through a reverse classification task where the probability of a sample being classified as class j is inversely proportional to its distance from O_j :

$$p(y = j | x, \mathcal{F}_\theta, O_j) = \frac{e^{d(\mathcal{F}_\theta(x), O_j)}}{\sum_{k=1}^N e^{d(\mathcal{F}_\theta(x), O_j)}}, \quad (6)$$

where d is the Euclidean distance function. After obtaining the classification probability, the cross entropy loss function is used to train the model:

$$\mathcal{L}_b^-(x; \theta, O_j) = -\log p(y = k | x, \mathcal{F}_\theta, O_j), \quad (7)$$

the learned open weight O_j characterizes features outside class j 's domain, representing its unknown space. The matrix of all base classes' open weights is denoted as O . To reduce training overhead and improve DNPG model generalization, we fix the feature extractor during open weights learning, allowing only the open weights to be trainable.

Raw Class Prototypes Calibration Inspired by [14], we refine the raw class prototypes P^r for novel classes during the meta-learning phase using the base class weights P^* (refer to Figure 4, left). Specifically, we adjust P^r to incorporate characteristics akin to P^* , resulting in the final class prototypes P :

$$\mathbf{A}_{(P^r, P^*)} = \frac{1}{\sqrt{d}} \left(P^r W^q \left(P^* W^k \right)^T \right), \quad (8)$$

$$P = P^r + \sigma \left(\mathbf{A}_{(P^r, P^*)} \right) (P^* W^v), \quad (9)$$

where $W^q, W^k, W^v \in \mathbb{R}^{d \times d}$ are trainable parameters, and σ denotes the softmax operation. The resulting weight matrix $\mathbf{A}_{(P^r, P^*)} \in \mathbb{R}^{|C_S| \times |C_B|}$ captures the learned relationships between novel and base classes for task T .

Multiple NPs Generator Based on Open Weights The open weights, representing the unknown space of base classes, reveal

that samples from similar classes exhibit analogous characteristics in this space (discussed in the Appendix, Section B). Exploiting this observation, we generate Negative Prototypes (NPs) for novel classes using the open weights of base classes (see Figure 4, right).

Specifically, leveraging the class similarity matrix $\mathbf{A}_{(P^r, P^*)}$ from Eq. 8, we construct the NPs by allowing novel classes to mimic the unknown space characteristics of base classes, while preserving the class similarity relationships. The NPs for each novel class are generated as follows:

$$P^- = \sigma \left(\mathbf{A}_{(P^r, P^*)} \right) (OW^v), \quad (10)$$

where W^v is a trainable parameter, and O and $\mathbf{A}_{(P^r, P^*)}$ represent the open weights of base classes. Each NP, $P_j^- \in P^-$, signifies the negation of novel class j . To optimize P_j^- , we employ a binary cross-entropy loss that minimizes its similarity with queries of class j and maximizes its similarity with queries from other classes:

$$\begin{aligned} \mathcal{L}_n^{neg}(j) = & \frac{1}{|Q_k^j|} \sum_{q \in Q_k^j} \mathcal{L}_{BCE} \left(0, f_s \left(\mathcal{F}_\theta(q), P_j^- \right) \right) \\ & + \frac{1}{|Q_u|} \sum_{q \in Q_u} \mathcal{L}_{BCE} \left(1, f_s \left(\mathcal{F}_\theta(q), P_j^- \right) \right). \end{aligned} \quad (11)$$

Then, we utilize the NP $P_j^- \in P^-$ of each novel class to replace the input p_c^r in Eq. 4, resulting in the NP p^- for the entire task. Considering the diverse appearances of unknown samples (e.g., both dogs and tigers can be considered unknown for the 'cat' class), we propose employing multiple NPs for each task. Specifically, we apply N MLPs to Eq. 4, yielding N distinct NPs:

$$p_k^- = f_k^{mlp} \left(p_{avg}^- \right), \quad k \in \{1, \dots, N\}. \quad (12)$$

4.3 Swap Alignment Module

Although we have generated multiple NPs for each task, not all NPs are effective, as detailed in Section 5.4. To address this, we propose the Swap Alignment Module (SA) to facilitate the generation of diverse and suitable NPs for tasks involving different classes.

Inspired by ATT-G [18], we employ a conjugate method to sample a pair of tasks $\mathcal{T}_1 = (S^1, Q_k^1, Q_u^1 | C_k^1)$ and $\mathcal{T}_2 = (S^2, Q_k^2, Q_u^2 | C_k^2)$, with the property that $Q_k^1 = Q_u^2$ and $Q_u^1 = Q_k^2$. This implies that the known few-shot classes C_k^1 in \mathcal{T}_1 and C_k^2 in \mathcal{T}_2 serve as negative sources for each other. We refer to \mathcal{T}_1 and \mathcal{T}_2 as each other's swap tasks.

For these swap tasks, our model generates prototypes and NPs, denoted as $[P_1, P_1^-]$ and $[P_2, P_2^-]$, respectively. We then apply the swap alignment operations:

$$(P_{i,a}, P_{i,a}^-) = \text{GCN} \left(P_i, P_i^- \right), \quad i \in \{1, 2\}, \quad (13)$$

$$\begin{aligned} \mathcal{L}_n^{\text{align}} = & \sum_i \arg\max_j \text{sim} \left(P_{1,a}^{i,-}, P_{2,a}^j \right) \\ & + \sum_j \arg\max_i \text{sim} \left(P_{2,a}^j, P_{1,a}^{i,-} \right). \end{aligned} \quad (14)$$

The GCN is a lightweight GCN network used for information propagation between prototypes and NPs, $P_{2,a}^j$ is the prototype of the j -th novel class in task \mathcal{T}_2 , and $P_{1,a}^{i,-}$ is the i -th generated negative prototype in task \mathcal{T}_1 . For each pair of swap tasks, we minimize the

Table 1: Closed-set ACC and open-set AUROC on two datasets. For each test, 4800 tasks are randomly sampled to ensure a confidence interval within ± 0.3 .

Algorithm	Remark	MiniImageNet				TieredImageNet			
		5-way 1-shot		5-way 5-shot		5-way 1-shot		5-way 5-shot	
		ACC	AUROC	ACC	AUROC	ACC	AUROC	ACC	AUROC
PEELER	CVPR2020	58.31 \pm 0.58	61.66 \pm 0.62	61.66 \pm 0.62	61.66 \pm 0.62	-	-	-	-
PEELER-Res12	CVPR2020	65.86 \pm 0.85	65.86 \pm 0.85	65.86 \pm 0.85	65.86 \pm 0.85	69.51 \pm 0.92	65.20 \pm 0.76	84.10 \pm 0.66	73.27 \pm 0.71
SnaTCHer-F	CVPR2021	67.02 \pm 0.85	68.27 \pm 0.96	82.02 \pm 0.53	82.02 \pm 0.53	70.52 \pm 0.96	74.28 \pm 0.80	84.74 \pm 0.69	82.02 \pm 0.64
SnaTCHer-T	CVPR2021	66.60 \pm 0.80	70.17 \pm 0.88	81.77 \pm 0.53	76.66 \pm 0.78	70.45 \pm 0.95	74.84 \pm 0.79	84.42 \pm 0.68	82.03 \pm 0.66
SnaTCHer-L	CVPR2021	67.60 \pm 0.83	69.40 \pm 0.92	82.36 \pm 0.58	76.15 \pm 0.83	70.85 \pm 0.99	74.95 \pm 0.83	85.23 \pm 0.64	80.81 \pm 0.68
RFDNet-Res12	TMM2022	66.23 \pm 0.80	71.37 \pm 0.80	82.44 \pm 0.54	80.31 \pm 0.59	66.84 \pm 0.89	72.68 \pm 0.76	82.64 \pm 0.63	80.63 \pm 0.63
ATT	CVPR2022	67.64 \pm 0.81	71.35 \pm 0.68	82.31 \pm 0.49	79.85 \pm 0.58	69.34 \pm 0.95	72.74 \pm 0.78	83.82 \pm 0.63	78.66 \pm 0.65
ATT-G	CVPR2022	68.11 \pm 0.81	72.41 \pm 0.72	83.12 \pm 0.48	79.85 \pm 0.57	70.58 \pm 0.93	73.43 \pm 0.78	85.38 \pm 0.61	81.64 \pm 0.63
GEL	CVPR2023	68.26 \pm 0.85	73.70 \pm 0.82	83.05 \pm 0.55	82.29 \pm 0.60	70.50 \pm 0.93	75.86\pm0.81	84.60 \pm 0.65	81.95 \pm 0.72
ASOP-L	ICIP2023	67.85 \pm 0.20	71.91 \pm 0.70	82.81 \pm 0.30	81.04 \pm 0.20	71.49 \pm 0.40	75.04 \pm 0.40	85.15 \pm 0.10	81.51 \pm 0.10
DNPG	Ours	69.10\pm0.29	74.18\pm0.28	83.74\pm0.19	83.64\pm0.19	71.52\pm0.32	75.70\pm0.21	85.54\pm0.22	82.94\pm0.23

Table 2: Closed-set ACC and open-set AUROC on CIFAR-FS dataset.

Algorithm	5-way 1-shot		5-way 5-shot	
	ACC	AUROC	ACC	AUROC
PEELER-Res12	71.47 \pm 0.67	71.28 \pm 0.57	85.46 \pm 0.47	75.97 \pm 0.33
RFDNet-Res12	73.83 \pm 0.92	75.35 \pm 0.77	85.12 \pm 0.74	84.40 \pm 0.64
ATT-G	72.43 \pm 0.65	76.72 \pm 0.59	86.52 \pm 0.49	84.64 \pm 0.38
GEL	76.67 \pm 0.90	79.43 \pm 0.72	87.63 \pm 0.62	86.84 \pm 0.58
DNPG	77.26\pm0.30	80.83\pm0.19	88.68\pm0.20	87.90\pm0.13

distance between each negative prototype in \mathcal{T}_1 and the most similar novel prototype in \mathcal{T}_2 , and vice versa. This alignment ensures that the unknown classes in \mathcal{T}_1 (represented by the negative prototypes) correspond to the novel classes in \mathcal{T}_2 (represented by the prototypes). The alignment loss $\mathcal{L}_n^{\text{align}}$ aims to bring the NPs of task \mathcal{T}_1 closer to the prototypes of task \mathcal{T}_2 , as they represent the same set of samples ($Q_u^1 = Q_k^2$). By reducing the distance between NPs and prototypes, the NPs become more discriminative and better approximate the distribution of real samples.

For \mathcal{T}_1 in the swap task pair $(\mathcal{T}_1, \mathcal{T}_2)$, the final loss function is:

$$\mathcal{L}_{\mathcal{T}_1} = \mathcal{L}_{CE}(Q_k^1 \cup Q_u^1) + \alpha \mathcal{L}_n^{\text{neg}} + \beta \mathcal{L}_n^{\text{align}} \quad (15)$$

where α and β are hyperparameters. Similarly, we calculate $\mathcal{L}_{\mathcal{T}_2}$ for task \mathcal{T}_2 . The total swap training loss is $\mathcal{L} = \mathcal{L}_{\mathcal{T}_1} + \mathcal{L}_{\mathcal{T}_2}$.

5 EXPERIMENTS

5.1 Datasets and Implementation Details

Datasets. We conduct FSOR experiments are conducted on three widely-used few-shot learning datasets: MiniImageNet [40], TieredImageNet [32], and CIFAR-FS [3]. MiniImageNet is a subset of ILSVRC-12 [34], consisting of 100 categories with 600 images each. The dataset is divided into meta-training, meta-validation, and meta-testing sets with 64, 16, and 20 categories, respectively. TieredImageNet, also a subset of ILSVRC-12, contains 608 categories divided

into 351, 97, and 160 categories for the respective sets. CIFAR-FS is derived from CIFAR100 [22], comprising 60,000 images across 100 categories, with the same division scheme as MiniImageNet.

Implementation Details. Following the settings of GEL [41] and ATT-G [18], we employ ResNet-12 as the feature extractor. During the pre-training phase, we follow the protocol of Tian et al. [39] and Huang et al. [18], pre-training ResNet-12 and a linear classifier with a combination of cross-entropy loss and self-supervised rotation loss on the base set for 90 epochs. We use SGD as the optimizer, with an initial learning rate of 0.05, decayed by a factor of 10 at epoch 60. In the meta-training phase, the learning rate is set to 0.0001 for ResNet-12 and 0.05 for all other layers in the negative prototype generator. For FSOR testing and evaluation, we follow the task sampling strategy of Liu et al. [27], setting $N = 5$ and $K = 1, 5$. Each task includes 15 positive queries from each few-shot class and 5 negative classes, each with 15 negative queries. We employ cosine similarity as the similarity function, utilizing two different temperature coefficients for comparing samples with prototypes (sim1) and negative prototypes (sim2). Additionally, a trainable bias is added to sim2 , allowing for an adjustable similarity offset for all samples to the negative prototype. Classification into the sixth class (representing the unknown class) is based on Equation 3, with the sample's probability of belonging to this class determined accordingly. The hyperparameters α and β are both set to 1.

Metrics. Consistent with prior work [13, 18, 37, 41], we evaluate closed-set classification performance using the accuracy metric (ACC) and open-set recognition performance using the Area Under the ROC Curve (AUROC). Higher values of ACC and AUROC indicate superior performance.

5.2 Few-Shot Open-Set Recognition

We evaluate our model against state-of-the-art (SOTA) few-shot open-set recognition approaches, which can be categorized into two groups: Negative-Prototype-Based methods, including ATT, ATT-G [18], and ASOP-L [21], and threshold-based models, such as PEELER [27], SnaTCHer [20], RFDNet [13], and GEL [41]. Notably, PEELER and RFDNet originally employ Res-18 as the feature

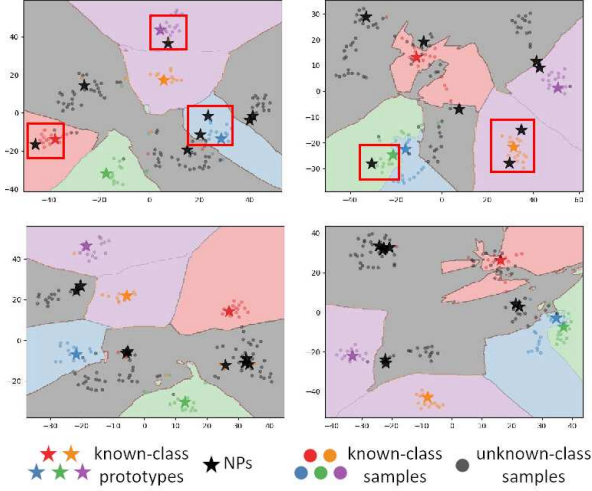


Figure 5: Visualization of prototypes and NPs for a 5-way 5-shot FSOR task on CIFAR-FS. The first row shows NPs by ATT-G, often inaccurately approximating known class prototypes (red boxes). The second row shows NPs by our DNPG, accurately representing unknown class space (gray background). Each column is a different episode.

extractor, but Wang et al. [41] implemented Res-12 versions, denoted as PEELER* and RFDNet*, whose results we directly quote for comparison. For other models, we use the results reported in their respective papers.

Tables 1 and 2 present our model’s performance compared to other approaches on three datasets. Our method surpasses all competing methods in both 1-shot and 5-shot settings across all datasets. It is important to note that the innovation of our model lies in its ability to learn unknowns from unknowns. This is highlighted by the fact that our model consistently outperforms the ATT-G model, which also utilizes information from both novel and base classes during testing, on all datasets. This indicates that our approach of learning unknowns from unknowns is indeed effective for the FSOR task. Given that the ATT-G model outperforms the ATT model, we select ATT-G as the representative of existing Negative-Prototype-Based FSOR models in subsequent experiments.

To further demonstrate the superiority of our DNPG model, we provide visualizations of prototypes and NPs generated by both the ATT-G and DNPG models in Figure 5. For both models, we set $N = 8$, meaning that 8 MLPs are used to generate 8 NPs for each task. It can be observed that the NPs generated by the ATT-G model, which relies on support samples as inputs, tend to erroneously converge towards the prototypes of the corresponding classes, thereby losing their ability to effectively model unknown samples. Conversely, our DNPG model does not suffer from this issue, maintaining the distinctiveness of NPs from the prototypes.

5.3 Ablation Study

To assess the contribution of each component in the DNPG model, we conducted an ablation study with $N = 5$, meaning that 5 MLPs are used to generate 5 NPs for each task. In this context, MNG

refers to the proposed NPs generator. Although the RPC module is not a novel contribution of our work, it is an integral part of our model; thus, for fairness, we also present results for the baseline combined with RPC. SA denotes the Swap Alignment Module. Since the SA module is designed based on Conjugate Training (CT) [18], we include an ablation model, baseline + RPC + MNG + CT, which excludes the SA module and solely employs conjugate training.

Table 3 shows the performance of each ablation model on the MiniImageNet dataset for 5-way 1-shot and 5-way 5-shot FSOR tasks. The results demonstrate that the DNPG model significantly outperforms the baseline in both ACC and AUROC metrics. Additionally, each individual module contributes positively to the overall performance of the model.

By comparing the baseline + RPC + MNG + CT model with the baseline + RPC + MNG + SA model, it is evident that conjugate training does not markedly enhance our model. This is because conjugate training is aimed at mitigating the overfitting of generated NPs to the pseudo-unknown class samples. However, our model does not rely on pseudo-unknown class samples for generating NPs, thereby circumventing the overfitting issue. In contrast, the SA module significantly boosts the performance of our model, underscoring its importance in the DNPG framework.

Table 3: Ablation study of our model. We report the 5-way 1-shot and 5-way 5-shot results on MiniImageNet. Our innovations are bolded.

Method	5-way 1-shot		5-way 5-shot	
	Acc	AUROC	ACC	AUROC
baseline	65.16±0.29	71.32±0.28	81.65±0.19	78.96±0.23
baseline + RPC	66.66±0.29	71.94±0.29	81.77±0.20	77.99±0.24
baseline + RPC + MNG	68.24±0.29	73.54±0.27	83.34±0.19	82.44±0.20
baseline + RPC + MNG + CT	68.22±0.29	73.48±0.28	83.33±0.19	82.44±0.18
baseline + RPC + MNG + SA	69.1±0.29	74.18±0.28	83.75±0.19	83.63±0.19

5.4 Further Analysis

Better Negative Prototypes, Wider Unknown Space. To further validate that our model’s NPs contain minimal known class information and can model a broader unknown space, we conduct experiments using two distinct datasets to generate NPs and analyze their differences.

We train three FSOR models, ATT-G [18], GEL [41], and our DNPG, on the training set of MiniImageNet. After fixing all parameters, we evaluate the models on both the test set of MiniImageNet and the test set of CIFAR-FS. We apply Principal Component Analysis (PCA) to reduce the dimensionality of the generated NPs in ATT-G and DNPG and visualize them. Since GEL is not a Negative-Prototype-Based model, it does not generate NPs.

Figures 6a and 6b show the distributions of prototypes and NPs generated by the ATT-G and DNPG models for both MiniImageNet and CIFAR-FS datasets. The NPs generated by the ATT-G model display noticeable differences between the two datasets, indicating the incorporation of dataset-specific information. In contrast, our DNPG model produces universal NPs that effectively model a wide range of unknown spaces, making it difficult to distinguish the learned NPs between the two datasets.

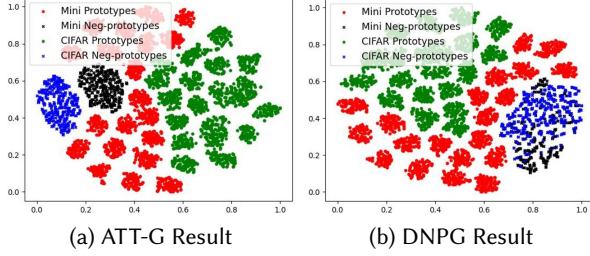


Figure 6: (a) The ATT-G model generated prototypes and NPs for both MiniImagenet and CIFAR-FS, which exhibit distinct differences between the two datasets due to the incorporation of dataset-specific information, and limited to a very small part of the space. (b) Our DNPG model generated prototypes and NPs for both MiniImagenet and CIFAR-FS, which are more indistinguishable and model a larger part of the space.

Lastly, we compare the ability of different models to fit unknown class data using the learned NPs. Specifically, we calculate the maximum similarity between each unknown class sample and the NPs during testing. The results indicate that the average similarity of the NPs generated by DNPG to unknown class samples is above 0.7, whereas ATT-G has only around 0.55 (similarity distribution histogram can be found in the Appendix.). This demonstrates that the NPs learned by our model exhibit superior ability to fit various unknown class samples, further validating the effectiveness of our approach.

How does the SA Module Work? To enhance the model’s adaptability to tasks composed of diverse data, we generate multiple NPs for each task. Existing methods, such as ATT-G [18], use the distance between a sample and its most similar NP as the classification score for the unknown class during both training and testing. However, simply employing multiple NPs does not ensure sufficient differentiation among them to effectively model samples from different unknown classes. In our experiments, we observed that some NPs tend to converge, collapsing to the same point in the unknown space, resulting in underutilization of the NPs.

We incrementally increase the hyperparameter N (the number of generated NPs) from 1 to 8 and record the changes in model performance with (w) and without (wo) the SA module. Simultaneously, we track the number of NPs that are utilized at least once during the entire testing process. The results, depicted in Figure 7, reveal that without the SA module, the model can effectively use up to 3 NP generators. With the SA module, the model can fully utilize each generator, and the performance improves with the growth of N until $N = 5$, where the best model performance is achieved.

Some models attempt to address the issue of collapsing by incorporating an equipartition constraint [31, 42], which introduces a fixed-sized feature space for prototype assignment. However, in our experiments, we found that this approach fails to resolve the collapsing problem in the FSOR task. In both the DNPG model and the model without the SA module (DNPG - SA), we applied the equipartition constraint, similar to the method outlined in [31, 42], to restrict the number of negative prototypes matching with samples. The results, as shown in Table 4, indicate that adding the

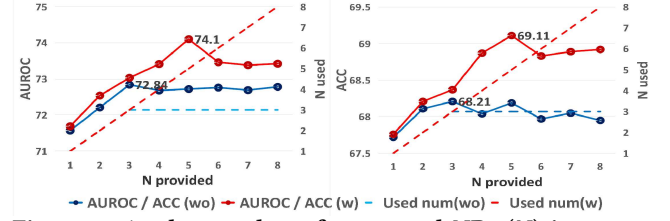


Figure 7: As the number of generated NPs (N) increases. When the SA module is not used, only a maximum of 3 NPs will actually be used (blue dashed line), after using the SA module, each NP can be used (red dashed line), and the effect is further improved (the red line continues to rise).

equipartition constraint negatively affects the model’s performance on the FSOR task. In FSOR task, forcing each negative prototype to match in every episode is not suitable because the composition of known and unknown classes continuously varies across episodes. In certain cases, the unknown classes may consist of a similar set of classes, such as “Dalmatian” and “Alaskan Malamute.” In such instances, it is more appropriate to allow the same negative prototype to represent them instead of forcing the use of a completely dissimilar negative prototype. This issue does not arise in our SA module, as we enable automatic matching between prototypes and negative prototypes, providing greater flexibility.

Table 4: When adding the equipartition constraint (EC) to our DNPG model (both with and without the SA module), the changes in the 5-way 1-shot ACC and AUROC on the miniImageNet dataset.

	ACC	AUROC
DNPG - SA	67.96±0.31	72.74±0.21
DNPG - SA + EC	67.62±0.27	72.15±0.19
DNPG	69.10±0.29	74.18±0.28
DNPG + EC	67.70±0.32	72.40±0.21

5.5 Conclusion

In this paper, we investigate the task of few-shot open-set recognition. To generate diversified negative prototypes for identifying unknown class samples, we propose the DNPG model. DNPG decouples the known class sample information from the generation of negative prototypes. Instead, DNPG transfers the information learned from the unknown representation on the base classes to generate negative prototypes corresponding to novel classes. This approach ensures that the generated negative prototypes do not contain excessive known class sample information, thereby covering a broader range of unknown spaces. To ensure that each negative prototype has a certain performance and models the unknown space from different directions, we introduce the SA module, which guaranteed that multiple NPs will not collapse to the same point in the unknown space. Extensive experiments validate the effectiveness of our approach.

ACKNOWLEDGMENTS

This work is supported by the National Natural Science Foundation of China under grants 62206102, 62376103, 62302184, and U1936108; the Science and Technology Support Program of Hubei Province under grant 2022BAA046; the Postdoctoral Fellowship Program of CPSF under grants GZB20230024 and GZC20240035; and the China Postdoctoral Science Foundation under grant 2024M750100.

REFERENCES

- [1] Antreas Antoniou, Harrison Edwards, and Amos Storkey. 2018. How to train your MAML. *arXiv preprint arXiv:1810.09502* (2018).
- [2] Abhijit Bendale and Terrance E Boulton. 2016. Towards open set deep networks. In *Proceedings of the IEEE conference on computer vision and pattern recognition*. 1563–1572.
- [3] Luca Bertinetto, Joao F Henriques, Philip HS Torr, and Andrea Vedaldi. 2018. Meta-learning with differentiable closed-form solvers. *arXiv preprint arXiv:1805.08136* (2018).
- [4] Qi Cai, Yingwei Pan, Ting Yao, Chenggang Yan, and Tao Mei. 2018. Memory matching networks for one-shot image recognition. In *Proceedings of the IEEE conference on computer vision and pattern recognition*. 4080–4088.
- [5] Yongjuan Che, Yuxuan An, and Hui Xue. 2023. Boosting few-shot open-set recognition with multi-relation margin loss. In *Proceedings of the Thirty-Second International Joint Conference on Artificial Intelligence*. 3505–3513.
- [6] Guangyao Chen, Siwei Dong, Yu Shu, Ge Zhang, Jaward Sesay, Börje F Karlsson, Jie Fu, and Yemin Shi. 2024. Autoagents: A framework for automatic agent generation. In *Proceedings of the International Joint Conference on Artificial Intelligence*.
- [7] Guangyao Chen, Peixi Peng, Yangru Huang, Mengyue Geng, and Yonghong Tian. 2024. Adaptive Discovering and Merging for Incremental Novel Class Discovery. In *Proceedings of the AAAI Conference on Artificial Intelligence*, Vol. 38. 11276–11284.
- [8] Guangyao Chen, Peixi Peng, Xiangqian Wang, and Yonghong Tian. 2021. Adversarial reciprocal points learning for open set recognition. *IEEE Transactions on Pattern Analysis and Machine Intelligence* 44, 11 (2021), 8065–8081.
- [9] Guangyao Chen, Limeng Qiao, Yemin Shi, Peixi Peng, Jia Li, Tiejun Huang, Shiliang Pu, and Yonghong Tian. 2020. Learning open set network with discriminative reciprocal points. In *Computer Vision—ECCV 2020: 16th European Conference, Glasgow, UK, August 23–28, 2020, Proceedings, Part III* 16. Springer, 507–522.
- [10] Jiaqi Chen, Jiachen Lu, Xiatian Zhu, and Li Zhang. 2023. Generative semantic segmentation. In *Proceedings of the IEEE/CVF Conference on Computer Vision and Pattern Recognition*. 7111–7120.
- [11] Wei Chen, Yu Liu, Weiping Wang, Erwin M Bakker, Theodoros Georgiou, Paul Fieguth, Li Liu, and Michael S Lew. 2022. Deep learning for instance retrieval: A survey. *IEEE Transactions on Pattern Analysis and Machine Intelligence* (2022).
- [12] Marco Cuturi. 2013. Sinkhorn distances: Lightspeed computation of optimal transport. *Advances in neural information processing systems* 26 (2013).
- [13] Shule Deng, Jin-Gang Yu, Zihao Wu, Hongxia Gao, Yansheng Li, and Yang Yang. 2022. Learning relative feature displacement for few-shot open-set recognition. *IEEE Transactions on Multimedia* (2022).
- [14] Spyros Gidaris and Nikos Komodakis. 2018. Dynamic few-shot visual learning without forgetting. In *Proceedings of the IEEE conference on computer vision and pattern recognition*. 4367–4375.
- [15] Guangxing Han, Jiawei Ma, Shiyuan Huang, Long Chen, and Shih-Fu Chang. 2022. Few-shot object detection with fully cross-transformer. In *Proceedings of the IEEE/CVF conference on computer vision and pattern recognition*. 5321–5330.
- [16] Guangxing Han, Xuan Zhang, and Chongrong Li. 2017. Revisiting faster r-cnn: A deeper look at region proposal network. In *Neural Information Processing: 24th International Conference, ICONIP 2017, Guangzhou, China, November 14–18, 2017, Proceedings, Part III* 24. Springer, 14–24.
- [17] Guangxing Han, Xuan Zhang, and Chongrong Li. 2018. Semi-supervised dff: Decoupling detection and feature flow for video object detectors. In *Proceedings of the 26th ACM international conference on Multimedia*. 1811–1819.
- [18] Shiyuan Huang, Jiawei Ma, Guangxing Han, and Shih-Fu Chang. 2022. Task-adaptive negative envision for few-shot open-set recognition. In *Proceedings of the IEEE/CVF Conference on Computer Vision and Pattern Recognition*. 7171–7180.
- [19] Muhammad Abdullah Jamal and Guo-Jun Qi. 2019. Task agnostic meta-learning for few-shot learning. In *Proceedings of the IEEE/CVF Conference on Computer Vision and Pattern Recognition*. 11719–11727.
- [20] Minki Jeong, Seokeon Choi, and Changick Kim. 2021. Few-shot open-set recognition by transformation consistency. In *Proceedings of the IEEE/CVF Conference on Computer Vision and Pattern Recognition*. 12566–12575.
- [21] Byeonggeun Kim, Jun-Tae Lee, Kyuhong Shim, and Simyung Chang. 2023. Task-Agnostic Open-Set Prototype for Few-Shot Open-Set Recognition. In *2023 IEEE International Conference on Image Processing (ICIP)*. IEEE, 31–35.
- [22] Alex Krizhevsky, Vinod Nair, and Geoffrey Hinton. 2010. Cifar-10 (canadian institute for advanced research). URL <http://www.cs.toronto.edu/kriz/cifar.html> 5, 4 (2010), 1.
- [23] Kimin Lee, Honglak Lee, Kibok Lee, and Jinwoo Shin. 2017. Training confidence-calibrated classifiers for detecting out-of-distribution samples. *arXiv preprint arXiv:1711.09325* (2017).
- [24] Xudong Li, Timin Gao, Xiaowu Zheng, Runze Hu, Jingyuan Zheng, Yunhang Shen, Ke Li, Yutao Liu, Pingyang Dai, Yan Zhang, and Rongrong Ji. 2024. Adaptive Feature Selection for No-Reference Image Quality Assessment using Contrastive Mitigating Semantic Noise Sensitivity. In *International Conference on Machine Learning*. PMLR, Vienna, Austria.
- [25] XuDong Li, Runze Hu, Jingyuan Zheng, Yan Zhang, Shengchuan Zhang, Xiaowu Zheng, Ke Li, Yunhang Shen, Yutao Liu, Pingyang Dai, et al. 2024. Integrating Global Context Contrast and Local Sensitivity for Blind Image Quality Assessment. In *International Conference on Machine Learning*. PMLR, Vienna, Austria.
- [26] Chen Liang, Wenguan Wang, Jiaxu Miao, and Yi Yang. 2022. Gmmseg: Gaussian mixture based generative semantic segmentation models. *Advances in Neural Information Processing Systems* 35 (2022), 31360–31375.
- [27] Bo Liu, Hao Kang, Haoxiang Li, Gang Hua, and Nuno Vasconcelos. 2020. Few-shot open-set recognition using meta-learning. In *Proceedings of the IEEE/CVF Conference on Computer Vision and Pattern Recognition*. 8798–8807.
- [28] Nikhil Mishra, Mostafa Rohaninejad, Xi Chen, and Pieter Abbeel. 2017. A simple neural attentive meta-learner. *arXiv preprint arXiv:1707.03141* (2017).
- [29] Sayak Nag, Dripta S Raychaudhuri, Sujay Paul, and Amit K Roy-Chowdhury. 2023. Reconstruction guided meta-learning for few shot open set recognition. *IEEE Transactions on Pattern Analysis and Machine Intelligence* (2023).
- [30] Wensheng Pan, Timin Gao, Yan Zhang, Xiaowu Zheng, Yunhang Shen, Ke Li, Runze Hu, Yutao Liu, and Pingyang Dai. 2024. Semi-Supervised Blind Image Quality Assessment through Knowledge Distillation and Incremental Learning. In *Thirty-Eighth AAAI Conference on Artificial Intelligence*. AAAI, Vancouver, Canada.
- [31] Zheyun Qin, Cheng Han, Qifan Wang, Xiushan Nie, Yilong Yin, and Xiankai Lu. 2023. Unified 3D Segmenter As Prototypical Classifiers. In *Thirty-seventh Conference on Neural Information Processing Systems*.
- [32] Mengye Ren, Eleni Triantafillou, Sachin Ravi, Jake Snell, Kevin Swersky, Joshua B Tenenbaum, Hugo Larochelle, and Richard S Zemel. 2018. Meta-learning for semi-supervised few-shot classification. *arXiv preprint arXiv:1803.00676* (2018).
- [33] Kaspar Riesen and Horst Bunke. 2008. IAM graph database repository for graph based pattern recognition and machine learning. In *Structural, Syntactic, and Statistical Pattern Recognition: Joint IAPR International Workshop, SSPR & SPR 2008, Orlando, USA, December 4–6, 2008, Proceedings*. Springer, 287–297.
- [34] Olga Russakovsky, Jia Deng, Hao Su, Jonathan Krause, Sanjeev Satheesh, Sean Ma, Zhiheng Huang, Andrej Karpathy, Aditya Khosla, Michael Bernstein, et al. 2015. Imagenet large scale visual recognition challenge. *International journal of computer vision* 115 (2015), 211–252.
- [35] Walter J Scheirer, Anderson de Rezende Rocha, Archana Sapkota, and Terrance E Boulton. 2012. Toward open set recognition. *IEEE transactions on pattern analysis and machine intelligence* 35, 7 (2012), 1757–1772.
- [36] Jake Snell, Kevin Swersky, and Richard Zemel. 2017. Prototypical networks for few-shot learning. *Advances in neural information processing systems* 30 (2017).
- [37] Nan Song, Chi Zhang, and Guosheng Lin. 2022. Few-shot open-set recognition using background as unknowns. In *Proceedings of the 30th ACM International Conference on Multimedia*. 5970–5979.
- [38] Liang-Yu Sun and Wei-Ta Chu. [n.d.]. Overall Positive Prototype for Few-Shot Open-Set Recognition. Available at SSRN 4617172 ([n.d.]).
- [39] Yonglong Tian, Yue Wang, Dilip Krishnan, Joshua B Tenenbaum, and Phillip Isola. 2020. Rethinking few-shot image classification: a good embedding is all you need?. In *Computer Vision—ECCV 2020: 16th European Conference, Glasgow, UK, August 23–28, 2020, Proceedings, Part XIV* 16. Springer, 266–282.
- [40] Oriol Vinyals, Charles Blundell, Timothy Lillicrap, Daan Wierstra, et al. 2016. Matching networks for one shot learning. *Advances in neural information processing systems* 29 (2016).
- [41] Haoyu Wang, Guansong Pang, Peng Wang, Lei Zhang, Wei Wei, and Yanning Zhang. 2023. Glocal Energy-based Learning for Few-Shot Open-Set Recognition. In *Proceedings of the IEEE/CVF Conference on Computer Vision and Pattern Recognition*. 7507–7516.
- [42] Wenguan Wang, Cheng Han, Tianfei Zhou, and Dongfang Liu. 2022. Visual recognition with deep nearest centroids. *arXiv preprint arXiv:2209.07383* (2022).
- [43] Yan Wang, Wei-Lun Chao, Kilian Q Weinberger, and Laurens Van Der Maaten. 2019. SimpleShot: Revisiting nearest-neighbor classification for few-shot learning. *arXiv preprint arXiv:1911.04623* (2019).
- [44] Shaoling Wu, HuiLan Luo, and Xiaomeng Lin. [n.d.]. TNPNet: An Approach to Few-Shot Open-Set Recognition via Contextual Transductive Learning. Available at SSRN 4592647 ([n.d.]).
- [45] Hongjie Zhang, Ang Li, Jie Guo, and Yanwen Guo. 2020. Hybrid models for open set recognition. In *Computer Vision—ECCV 2020: 16th European Conference, Glasgow, UK, August 23–28, 2020, Proceedings, Part III* 16. Springer, 102–117.

- [46] Jikui Zhao, Huaxia Wang, Shengliang Peng, and Yu-Dong Yao. 2024. Meta Supervised Contrastive Learning for Few-Shot Open-Set Modulation Classification with Signal Constellation. *IEEE Communications Letters* (2024).
- [47] Da-Wei Zhou, Han-Jia Ye, and De-Chuan Zhan. 2021. Learning placeholders for open-set recognition. In *Proceedings of the IEEE/CVF conference on computer vision and pattern recognition*. 4401–4410.
- [48] Yixiong Zou, Shanghang Zhang, Guangyao Chen, Yonghong Tian, Kurt Keutzer, and José MF Moura. 2021. Annotation-Efficient Untrimmed Video Action Recognition. In *Proceedings of the 29th ACM International Conference on Multimedia*. 487–495.

In this Appendix, additional experiment results are presented. Also, we evaluated the computational and storage overheads of the DNPG model.

A MORE FSOR RESULT.

Additionally, on the COIL-DEL graph dataset [33], our model demonstrates strong FSOR performance, as shown in Table 5.

Table 5: The 5-way 1-shot FSOR result on the COIL-DEL dataset, which is commonly used for graph classification tasks.

	ACC	AUROC
ATT-G	75.24	76.70
baseline	73.20	73.41
DNPG (ours)	75.51	77.25

B THE EXPRESSIVE POWER OF THE OPEN WEIGHTS

Figure 8 shows the similarity heatmaps between base classes using both base weights and open weights. The open weights effectively capture the inter-class similarity relationships, similar to the base weights. This demonstrates the expressive power of the open weights in representing unknown spaces. Consequently, we propose using open weights to generate NP.

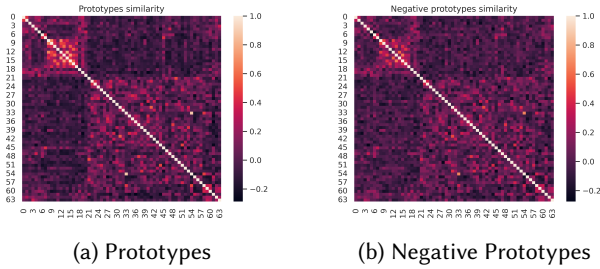


Figure 8: Heatmap visualization of cosine similarity between classes. (a) shows similarity using class prototypes, and (b) displays similarity between negative prototypes learned by RPL [9]. Both approaches yield highly concordant similarity relationships.

C BETTER NEGATIVE PROTOTYPE

Firstly, in Figure 9, we provide a more comprehensive illustration than the main text Figure 5. It can be observed that existing Negative-Prototype-Based FSOR models indeed suffer from the issue of erroneously approximating negative prototypes to known class representations, thus failing to model unknown samples. Our model effectively addresses this issue.

We further complement our analysis with Figure 7 in the paper to illustrate why our approach of “learning unknowns from unknowns” leads to superior negative prototype generation. In Figure

7, it can be observed that the negative prototypes generated by the ATT-G model for different datasets are completely separated. This is because the approach of generating negative prototypes based on known sample information leads to distinct and separate negative prototypes when input samples differ. In contrast, our model first generates representations of the unknown space, and then uses only these learned representations in downstream tasks to generate negative prototypes. This approach, which is not directly linked to current input information, results in negative prototypes that are less influenced by input samples, but instead are more generalizable and difficult to distinguish, as depicted in Figure 7. Additionally, it can be observed that the coverage range of the negative prototypes generated by our model is greater than that of the ATT-G model. This subjective analysis explains why our approach to negative prototype generation is superior to existing methods.

On an objective level, we provide the FSOR task performance of various models involved in plotting Figure 7 on two datasets, as shown in Table 6. It can be seen that the performance of our DNPG model on both datasets is significantly better than that of the ATT-G model. Furthermore, comparing the performance on the training dataset with that on the new dataset also reveals that the performance drop of our model when transferred to a new dataset is smaller than that of other models. This objectively demonstrates that our approach to generating negative prototypes leads to better FSOR model performance.

Table 6: 5-way 5 shot test results on TieredImageNet and CIFAR-FS, using ATT-G, GEL, and DNPG(ours) trained on TieredImageNet. Δ indicates degradation of the model’s effect before and after the model is migrated to test on CIFAR-FS, and smaller values indicate a more robust model.

Algorithm	TieredImageNet		CIFAR-FS		$\downarrow \Delta$	
	Acc	AUROC	ACC	AUROC	ACC	AUROC
ATT-G	84.54 \pm 0.67	78.84 \pm 0.76	72.64 \pm 0.73	61.39 \pm 0.68	11.9	17.5
GEL	83.55 \pm 0.72	81.06 \pm 0.72	62.19 \pm 0.71	61.60 \pm 0.63	21.4	19.4
DNPG	84.71\pm0.69	83.20\pm0.64	73.87\pm0.72	71.12\pm0.66	10.9	12.8

D MODEL ROBUST

Table 7: Our model is compared with the state-of-the-art model ATT-G [18] on the miniImageNet dataset with the addition of three types of noise, evaluating the 5-way 5-shot classification performance.

	blur	digital	extra	Average
ATT-G [18]	45.98 \pm 0.66	54.23 \pm 0.76	36.75 \pm 0.67	45.65
DNPG(ours)	49.98\pm0.68	58.39\pm0.70	39.39\pm0.69	49.25

We further show the robustness of our model under different conditions. Firstly, we evaluated the FSOR task performance of our model, DNPG, and the ATT-G model (one of the Negative-Prototype-Based SOTA FSOR models) on the miniImageNet dataset with the addition of three types of noise. The results are shown in

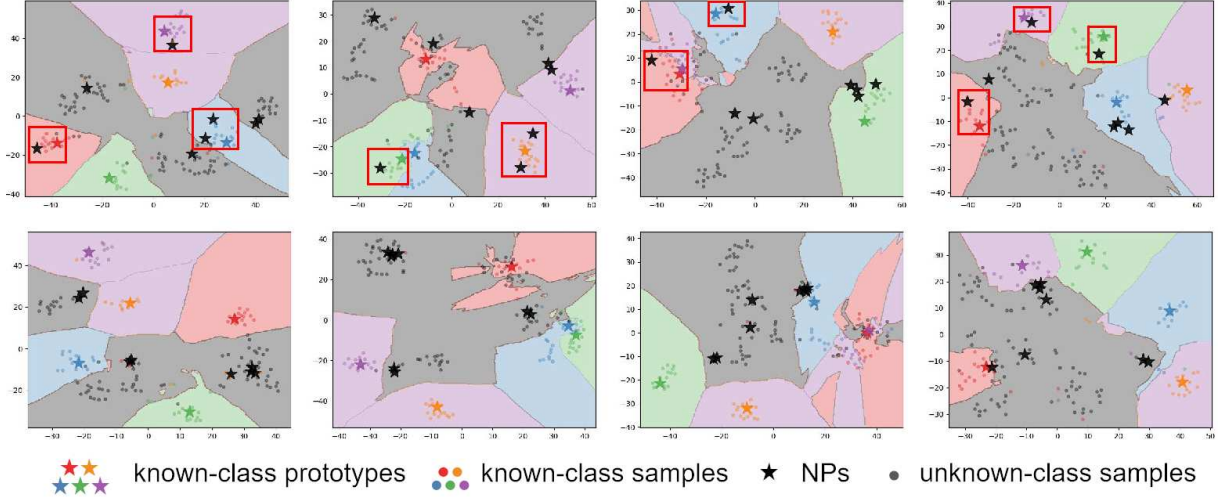


Figure 9: The visualization of the prototypes and NPs generated by one state-of-the-art method, ATT-G (the first line) and our DNPG models (the second line) in the 5-way-5-shot FSOR task on the CIFAR-FS dataset. Each column corresponds to a specific episode. The NPs generated by ATT-G incorrectly approximate the prototypes of known classes (highlighted in the red box). In contrast, the NPs generated by our model accurately model the space of unknown class samples (gray background area).

Table 8: The 5-way 1-shot performance of our model and an existing SOTA model ATT-G [18] on FSOR tasks under different class number settings.

Number of test classes	DNPG (ours)		ATT-G [18]		Δ	
	Acc	AUROC	ACC	AUROC	ACC	AUROC
5 novel + 5 unknown	68.83 \pm 0.85	73.62 \pm 0.79	67.33 \pm 0.85	72.11 \pm 0.78	1.50	1.51
6 novel + 6 unknown	64.81 \pm 0.75	71.52 \pm 0.71	63.30 \pm 0.76	70.02 \pm 0.71	1.51	1.50
7 novel + 7 unknown	61.13 \pm 0.71	70.56 \pm 0.69	59.71 \pm 0.72	68.86 \pm 0.68	1.42	1.70
8 novel + 8 unknown	58.30 \pm 0.64	69.19 \pm 0.59	56.75 \pm 0.64	67.43 \pm 0.60	1.55	1.76
9 novel + 9 unknown	55.54 \pm 0.60	68.62 \pm 0.56	54.04 \pm 0.62	66.78 \pm 0.56	1.50	1.84
10 novel + 10 unknown	52.89 \pm 0.54	68.19 \pm 0.53	51.63 \pm 0.55	66.11 \pm 0.53	1.26	2.08

Table 7. It can be observed that our model outperforms the ATT-G model significantly on datasets with various added noise. This is because the process of generating negative prototypes in the ATT-G model heavily relies on the information of the known class samples, and the addition of noise greatly affects the quality of input samples, thus leading to poor quality negative prototypes. On the other hand, our model, by severing the direct connection between input information and negative prototype generation, is less affected. Furthermore, we present the FSOR task performance of our model and the ATT-G model under different numbers of classes, as depicted in Table 8. It can be seen that our model consistently outperforms the ATT-G model across various class configurations. Additionally, we observe that as the number of known and unknown classes increases, the superiority of our model over the ATT-G model also increases. This further illustrates that our model is capable of generating more generalized negative prototypes, enabling better performance in FSOR tasks with varying numbers of classes.

E STORAGE AND COMPUTATIONAL EXPENSES

Here, we have calculated the computational and storage cost for the 5-way 1-shot task on miniImageNet. While DNPG does increase the number of parameters somewhat, it does not significantly raise the computational cost, comparing with the ATT-G [18] model.

Mehod	Parameter	FLOPs	Inference Time	Traing Time	
				pre-train	meta-learn
ATT-G	19.8 M	705.67 G	0.096 (sec/episode)	200 (sec/epoch)	0.431 (sec/epoch)
DNPG	21.4 M	706.20 G	0.097 (sec/episode)	200 (sec/epoch)	0.438 (sec/epoch)

F HYPERPARAMETER.

The primary hyperparameters of DNPG are α and β (result shown in Figure 10). Increasing α enhances the influence of $\mathcal{L}_n^{\text{neg}}$, shifting the focus towards learning NP while reducing its ability to model

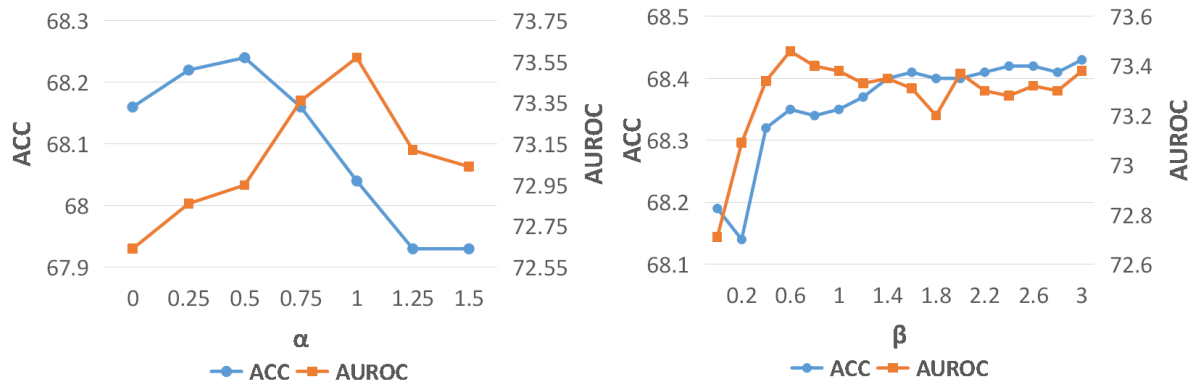


Figure 10: How the performance changes with the values of α and β .

prototypes, resulting in an antagonistic relationship between AUROC and ACC. Conversely, increasing β increases the importance of the SA, consistently and steadily improving the performance.